Reduction of proximity effect in fabricating nanometer-spaced nanopillars by two-step exposure*

Zhang Yang(张杨)[1, †], Zhang Renping(张仁平)[2], Han Weihua(韩伟华)[2], Liu Jian(刘剑)[1], Yang Xiang(杨香)[2],
Wang Ying(王颖)[2], Li Chian Chiu(李千秋)[3], and Yang Fuhua(杨富华)[1, 2]

(1 State Key Laboratory for Superlattices and Microstructures, Institute of Semiconductors, Chinese Academy of Sciences, Beijing 100083, China)

(2 Engineering Research Center for Semiconductor Integrated Technology, Institute of Semiconductors, Chinese Academy of Sciences, Beijing 100083, China)

(3 Department of Electronic Engineering, The Chinese University of Hong Kong, Hong Kong, China)

Abstract: A two-step exposure method to effectively reduce the proximity effect in fabricating nanometer-spaced nanopillars is presented. In this method, nanopillar patterns on poly-methylmethacrylate (PMMA) were partly cross-linked in the first-step exposure. After development, PMMA between nanopillar patterns was removed, and hence the proximity effect would not take place there in the subsequent exposure. In the second-step exposure, PMMA masks were completely cross-linked to achieve good resistance in inductively coupled plasma etching. Accurate pattern transfer of rows of nanopillars with spacing down to 40 nm was realized on a silicon-on-insulator substrate.

Key words: nanopillars; electron-beam lithography; negative PMMA; proximity effect

DOI: 10.1088/1674-4926/30/11/116001 **EEACC:** 2520

1. Introduction

As CMOS technology is constantly scaling down, studies on nanostructures[1−5] and nanodevices[6−9] have attracted much attention. Among them, nanostructures fabricated on a silicon-on-insulator (SOI) substrate with a top-down strategy are of particular interest. This is mainly due to their compatibility with CMOS technology and the superiority of SOI material over bulk silicon[10]. In the fabrication of nanostructures and nanodevices, electron-beam lithography (EBL) is probably the most prevalent method for transferring patterns.

Poly-methylmethacrylate (PMMA) is a commonly used resist in EBL. When irradiating it with electrons, two parallel processes occur. One is chain scission. This refers to the breaking down of PMMA molecules of high molecular weight into low molecular weight molecules. The other is cross-linking. This refers to the formation of a larger molecule network by creating short and strong covalent bonds between PMMA molecules. In general, when irradiated at low dose levels, the chain scission process dominates and PMMA behaves as a positive-tone resist. In contrast, when irradiated at high dose levels, the cross-linking process becomes dominant and PMMA turns to negative-tone. Therefore, PMMA can be used as either a positive-tone or negative-tone resist depending on the irradiation dose. Although PMMA is normally used as a positive-tone resist with high resolution, some work has also been done using PMMA as a negative-tone resist[11−15]. In these works, negative PMMA was employed as an insulating layer[11], an etching mask[12, 13], a gate dielectric and sacrificial layer in nano- and micro-electromechanical system fabrication[14], and a supporting post[15]. Like positive (degraded) PMMA, negative (cross-linked) PMMA also features high resolution. Furthermore, negative PMMA is more durable as it is subject to fluorine-based inductively coupled plasma (ICP) etching. In the negative PMMA process, the proximity effect, which is mainly caused by the backscattering of electrons, can be a serious issue due to the high irradiation dose[11, 13, 14]. The proximity effect can lead to the degradation of resolution. Zailer *et al.* proposed a technique involving two-stage exposure of PMMA to cope with the issue[11]. Nanometer-spaced nanostructures (e.g. a row of nanopillars) in isolating trenches are prevalent in building densely arrayed nanoscale devices. However, the technique proposed in Ref. [11] had some limitations in patterning such structures. To transfer such nanostructures accurately, one had to respectively assign appropriate doses for regions in between and far away from the nanostructure patterns in the first stage of exposure. This was nontrivial due to the complexity of electron dose distributions in these regions.

In this paper, the above-mentioned issue is circumvented by proposing a two-step exposure method. In the first-step exposure, nanopillar patterns are exposed to a dose level at which PMMA is partly cross-linked and the proximity effect is insignificant. Simultaneously, a box pattern is exposed at a standard dose to define the isolating trench. After development, PMMA in between nanopillar patterns is removed, and hence

---

* Project supported by the National Natural Science Foundation of China (Nos. 60506017, 60776059) and the National High Technology Research and Development Program of China (No. 2007AA03Z303).

† Corresponding author. Email: zhangyang@semi.ac.cn

Received 28 April 2009, revised manuscript received 12 June 2009

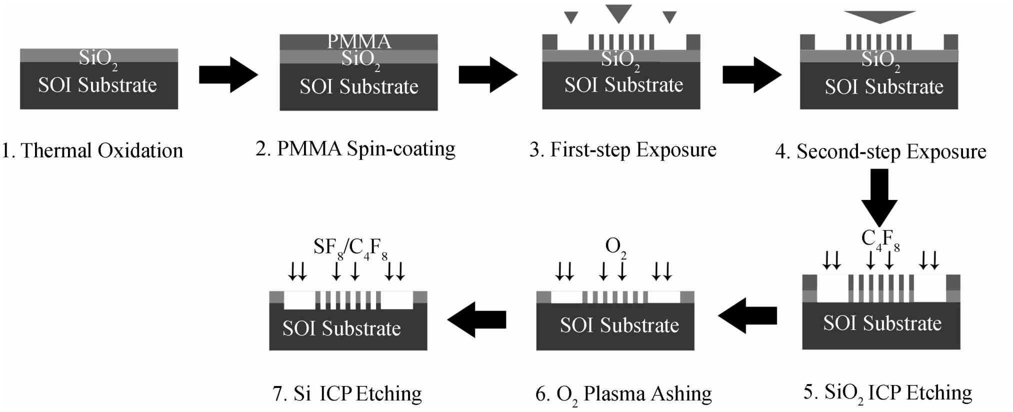

Fig. 1. Process flow for fabricating rows of nanopillars in isolating trenches on an SOI substrate.

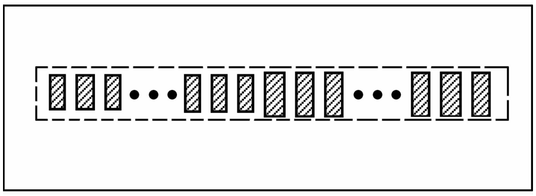

Fig. 2. Patterns designed for exposure of a row of nanopillars. The dots represent middle boxes that are not depicted in the schematic diagram.

no proximity effect takes place there in the next step of exposure. Subsequently, a second-step exposure is implemented to completely cross-link the PMMA and hence substantially increase its resistance to dry etching. Rows of nanopillar patterns with spacing down to 40 nm in isolating trenches are accurately transferred to the SOI substrate.

2. Experimental details

In this section, the fabrication of rows of nanopillars in isolating trenches on an SOI substrate will be described at length.

Figure 1 shows the process flow diagram of the fabrication. It started with the thermal growth of a 30-nm-thick SiO_2 layer on a cleaned SOI substrate. PMMA A2 (2% PMMA950K in anisole) was then spin-coated on the substrate at a speed of 5000 rpm for 50 s. Subsequently, the sample was baked on a hotplate at 180 °C for 2 min. The resultant thickness of the resist was about 63 nm. EBL was then carried out using a Raith150 system with an acceleration voltage of 10 kV. The aperture size and write-field were set to 30 μm and 100 μm, respectively. The patterns for exposure are depicted in Fig. 2. The outer solid-line box measured 8×2 μm^2. There were 40 hatched boxes in the middle of it. The first group of 20 hatched boxes ran from left to right, were 40 nm-evenly spaced, and each measured 80×190 nm^2. The remaining 20 hatched boxes formed the second group. They were 80 nm-evenly spaced and each measured 110×240 nm^2. The spacing between the two groups was 60 nm. In order to fabricate a row of nanopillars in an isolating trench, both the positive and negative processes of PMMA were adopted. The outer solid-line box and 40 hatched boxes were both exposed in the first-step exposure. The former was exposed at a low dose (1.4 C/m^2) to define the trench pattern, which utilized the positive process of PMMA. In contrast, the latter was exposed at a relatively high dose (200 C/m^2) to define nanopillar patterns. After the first-step exposure, the sample was developed for 20 s in a mixture of MIBK/IPA at a ratio of 1 : 3, then immersed in IPA for another 20 s and eventually blow-dried with nitrogen. Like the second-step exposure, the area surrounded by the dashed line was exposed at a dose of 280 C/m^2. Subsequently, the sample was subject to an ICP etch on an STS Multiplex AOE system to transfer patterns to the SiO_2 layer. The etching gas was a mixture of $C_4F_8/He/H_2$ at a ratio of 12 sccm : 174 sccm : 12 sccm. The ICP power and RF power used in the etching were 1000 W and 160 W, respectively. The experiment was conducted under a pressure of 4 mTorr for 28 s. The negative PMMA resist was thereafter removed in a Tepla microwave oxygen plasma asher. Finally, silicon etching was performed on an Alcatel 601E system with a gas mixture of SF_6/C_4F_8 (60 sccm/90 sccm) under a pressure of 1.8×10^{-2} mbar for 45 s. The ICP power and RF power used in the etching were 800 W and 120 W, respectively.

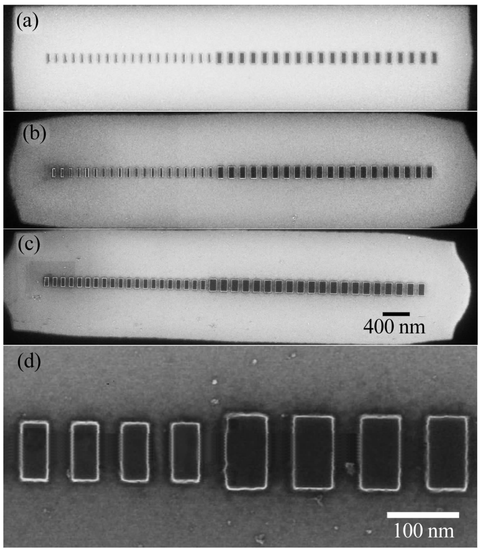

Fig. 3. (a)–(c) SEM images indicating nanopillar patterns exposed at doses of 64 C/m^2, 160 C/m^2 and 224 C/m^2, respectively; (d) The magnified image of (c).

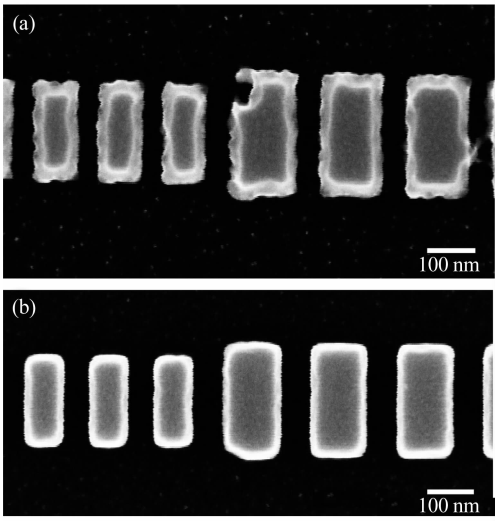

Fig. 4. SEM images demonstrating nanopillars fabricated with (a) the one-step exposure method and (b) two-step exposure method, respectively.

3. Results and discussion

For comparison, the one-step exposure method was also used to define rows of nanopillars. Figures 3(a) to 3(c) are scanning electron microscopy (SEM) images indicating nanopillar patterns on resist. They were exposed with doses of 64 C/m^2, 160 C/m^2 and 224 C/m^2, respectively. It can be seen that the patterns in Fig. 3(a) have blurred contours, while those in Figs. 3(b) and 3(c) have clear contours. However, as the exposure dose was as high as 224 C/m^2, the PMMA near the edges of nanopillar patterns had become partly cross-linked due to the proximity effect, as shown in Fig. 3(d). The partly cross-linked PMMA would serve as unwanted masks leading to severe edge roughness after ICP etching. Therefore the exposure dose should be in the range of 160 to 224 C/m^2 to achieve clear contours and avoid severe cross-linking in between nanopillars.

Figure 4(a) is an SEM image of nanopillars fabricated with the one-step exposure method. Nanopillar patterns in Fig. 4(a) were exposed at a dose of 480 C/m^2. This dose was sufficiently high to partly cross-link the PMMA between nanopillars via the proximity effect. Edge roughness was clearly demonstrated here. On the other hand, it was also observed in our experiments that nanopillar patterns on PMMA that were obtained at an exposure dose below 400 C/m^2 had poor selectivity to SiO$_2$ in step-5 in Fig. 1. This phenomenon is attributed to the incomplete cross-linking of PMMA. Obviously, there was a dilemma here. In order to obtain good masking ability, a dose higher than 400 C/m^2 was needed to expose the nanopillar patterns; on the other hand, the exposure dose must lie in the range mentioned above.

To circumvent this issue, a two-step exposure method was developed. As described in Section 2, a low dose (200 C/m^2), which would lead to no serious cross-linking of PMMA near the edges of nanopillar patterns, was applied to obtain patterns with clear contours on the PMMA resist. PMMA in between nanopillar patterns, which was actually exposed as a positive-tone resist in the trench pattern exposure, was removed after development. Consequently, as a second-step exposure was carried out to further cross-link the PMMA mask, there was no PMMA left to be cross-linked in between nanopillar patterns. Accordingly, detrimental consequences caused by the proximity effect in the one-step exposure were significantly reduced. The second-step exposure added 280 C/m^2 dosage to the gross dose and eventually made it 480 C/m^2. This step cross-linked the PMMA mask completely and hence substantially improved its masking ability.

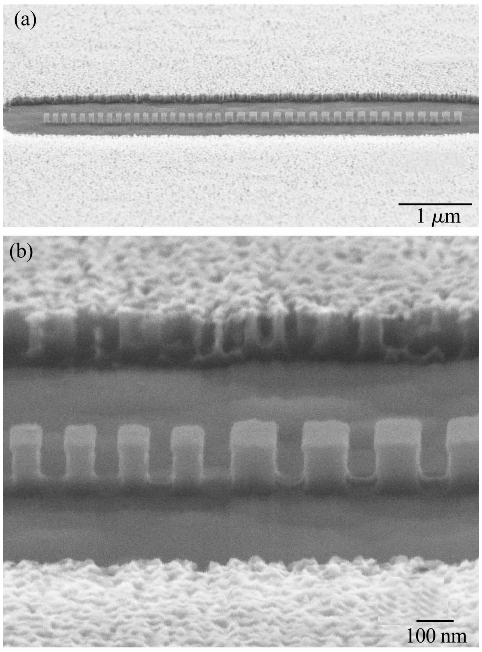

Fig. 5. SEM images indicating side views of nanopillars fabricated with the two-step exposure method taken at (a) low and (b) high magnifications, respectively.

The result obtained by utilizing the two-step exposure method is presented in Fig. 4(b). The smaller nanopillars were 80 nm in width and 190 nm in length. The larger ones measured 110 nm in width and 240 nm in length. This result indicated that the nanopillar patterns were accurately transferred from the negative PMMA masks to the SiO$_2$ layer. Moreover, smooth edges are clearly exhibited in the image. The spacing was 40 nm for the first group and 80 nm for the second group. Figures 5(a) and 5(b) are side-view SEM images taken at different magnifications. The height of the nanopillars is 166 nm. Slight undercuts in the silicon can be seen in Fig. 5(b), which widened the spacing a little. In addition, it can be seen that microtrenches between nanopillars had already been etched deep into the buried oxide layer. A row of nanopillars fabricated by the one-step exposure method on the same SOI substrate is shown in Fig. 6. However, microtrenches in this structure had not been etched into the buried oxide layer. This was ascribed to the masking effect of the partly cross-linked PMMA in between nanopillar patterns.

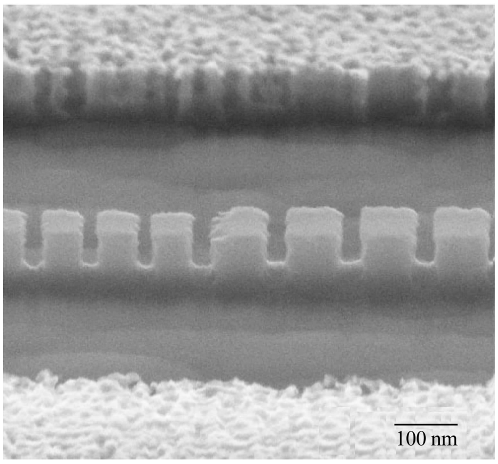

Fig. 6. SEM image showing side view of nanopillars fabricated with the one-step exposure method.

4. Conclusions

In summary, the detrimental consequences of the proximity effect were effectively reduced by the two-step exposure method in the fabrication of nanometer-spaced nanopillars in isolating trenches on the SOI substrate. In this method, nanopillar patterns on PMMA were partly cross-linked in the first-step exposure. After development, PMMA in between nanopillar patterns was removed, and hence there would be no proximity effect taking place there in the subsequent exposure. In the second-step exposure, PMMA masks were completely cross-linked to achieve good resistance in ICP etching. Accurate pattern transfer of rows of nanopillars with spacing down to 40 nm was achieved. The spacing can be further decreased if the spacing design in Fig. 2 is further reduced. Nanopillars fabricated in this work can be used in the study of nanoelectronic and nano-optoelectronic devices. Furthermore, the method proposed here can be used to fabricate other nanostructures that also suffer from issues caused by the proximity effect.

Acknowledgement

The authors thank Fan Zhongchao and Li Yan for helpful discussions.

References

[1] Nakata Y, Okada T, Maeda M. Fabrication of dot matrix, comb, and nanowire structures using laser ablation by interfered femtosecond laser beams. Appl Phys Lett, 2002, 88(22): 4239

[2] Lister K A, Casey B G, Dobson P S, et al. Pattern transfer of a 23 nm-period grating and sub-15 nm dots into CVD diamond. Microelectron Eng, 2004, 73/74: 319

[3] Chen Y F, Lu Z Q, Wang X D, et al. Fabrication of ferromagnetic nanoconstrictions by electron beam lithography using LOR/PMMA bilayer technique. Microelectron Eng, 2007, 84: 1499

[4] Han K S, Hong S H, Lee H. Fabrication of complex nanoscale structures on various substrates. Appl Phys Lett, 2007, 91: 123118

[5] Mukherjee P, Kang M G, Zurbuchen T H, et al. Fabrication of high aspect ratio Si nanogratings with smooth sidewalls for a deep UV-blocking particle filter. J Vac Sci Technol B, 2007, 25(6): 2645

[6] Tilke A T, Pescini L, Lorenz H, et al. Fabrication and transport characterization of a primary thermometer formed by Coulomb islands in a suspended silicon nanowire. Appl Phys Lett, 2003, 82(21): 3773

[7] Elibol O H, Morisette D, Akin D, et al. Integrated nanoscale silicon sensors using top-down fabrication. Appl Phys Lett, 2003, 83(22): 4613

[8] Khalafalla M A H, Ono Y, Nishiguchi K, et al. Identification of single and coupled acceptors in silicon nano-field-effect transistors. Appl Phys Lett, 2007, 91: 263513

[9] Chen Y F, Zhou Y, Wang L, et al. Nanofabrication of spintronic devices with ultra small ferromagnetic contacts. Microelectron Eng, 2008, 85(5/6): 1152

[10] Colinge J P. Silicon-on-insulator technology: materials to VLSI. Kluwer Academic Publishers, 1997

[11] Zailer I, Frost J E F, Chabasseur-Molyneux V, et al. Crosslinked PMMA as a high-resolution negative resist for electron beam lithography and applications for physics of low-dimensional structures. Semicond Sci Technol, 1996, 11: 1235

[12] Hoole A C F, Welland M E, Broers A N. Negative PMMA as a high-resolution resist-the limits and possibilities. Semicond Sci Technol, 1997, 12: 1166

[13] Ressier L, Grisolia J, Martin C, et al. Fabrication of planar cobalt electrodes separated by a sub-10nm gap using high resolution electron beam lithography with negative PMMA. Ultramicroscopy, 2007, 107: 985

[14] Teh W H, Liang C T, Graham M, et al. Cross-linked PMMA as a low-dimensional dielectric sacrificial layer. J Microelectromech Syst, 2003, 12(5): 641

[15] Borzenko T, Hock V, Supp D, et al. Building and testing submicrometer metallic (gold) air-bridges for nanotransport applications. Microelectron Eng, 2005, 78/79: 374